Photomedicine and Laser Surgery
Volume 30, Number 2, 2012

Pp. 85–91
DOI: 10.1089/pho.2011.3059

Raman Spectroscopic Investigation of the Effects of Cosmetic Formulations on the Constituents and Properties of Human Skin

Maira G. Tosato, M.Sc.,[1] Rani S. Alves, B.S.,[1] Edson A.P. dos Santos, B.S.,[1] Leandro Raniero, Ph.D.,[1] Priscila F.C. Menezes, Ph.D.,[2] Klésia M.S. Belletti, B.S.,[2] Carlos Eduardo O. Praes, B.S.,[2] and Airton A. Martin, Ph.D.[1]

Abstract

Objective: This study aimed to investigate the biochemical alterations in hydration and skin proteins, which are associated with the skin aging process, caused by cosmetic use. ***Background data:*** Many techniques have been used to assess the effectiveness of cosmetics' hydrating and anti-aging effects on skin. Recently, Raman spectroscopy has been shown to be a powerful, noninvasive tool that can monitor changes in the biomolecules of the skin in real time. ***Materials and methods:*** Were analyzed human skin *in vivo* at the beginning of the experiment (T0) and after 30 (T30) and 60 (T60) days of continuous use of a cosmetic product. Fourier-transform and dispersive Raman spectroscopy were the used to examine the periorbicular right lateral eye region of 16 female Brazilian volunteers, aged 60–75 years. Multivariate statistical analysis of principal components analysis (PCA) and linear discriminant analysis were performed on all Raman spectra. ***Results:*** Using the cosmetic product for 30 days increased the intensity of the Raman bands for collagen, amide III (1250–1350 cm^{-1}) for proteins, and the water (OH) stretching mode at 3250 cm^{-1}, suggesting that the treatment was effective. The changes observed at T30 were not sustained at the same intensity for 60 days. Intensity variations in other bands may be related to changes in the organization of the epidermis at the dermal matrix. ***Conclusions:*** The application of cosmetics with active moisturizing and anti-aging properties helps to maintain the skin's protective barrier and to slow the intrinsic and extrinsic aging processes of the skin.

Introduction

Skin is a biological interface with the environment and is highly metabolic, possesses the largest surface area of any organ in the human body,[1] and is composed of multiple layers differing in molecular composition and function. Cosmetic products are commonly used to help maintain skin homeostasis, sustaining the skin's water concentration and minimizing the effects of aging. Monitoring biomolecules' changes that occur after applying cosmetic ointments or creams is crucial to evaluating the efficacy of these products and/or treatments.

According to the Food and Drug Administration (FDA), cosmetics are defined as substances obtained from animal, vegetable, or mineral sources that do not cause physiological alterations upon permeation. Most cosmetic products penetrate into the stratum corneum, epidermis, and even the dermis, depending upon the physicochemical characteristics of the molecules and the use of permeation promoters, or delivery systems. [2–4]

Currently, the use of cosmetics is increasing, principally because of their ability to protect against ultraviolet (UV) radiation, delay extrinsic aging, and prevent intrinsic chronological aging.

The natural aging process of skin results in biological changes that mainly occur because of decreases in the dermal–epidermal interface. This decrease affects nutrient transport between the skin's layers, decreasing the extracellular matrix, inducing fragmentation of elastic fibers,[5] and promoting reduction of collagen synthesis by impairing fibroblast activity.[6] This process decreases the hydration affecting the performance of the protective barrier of the skin.[7,8] Rhie et al. described enzymatic and nonenzymatic changes that arise in the epidermis and dermis during the

[1]Laboratory of Biomedical Vibrational Spectroscopy, Institute of Research and Development (IP&D), University of the Vale do Paraíba, São José dos Campos, Brazil.
[2]O Boticário Franchising , Afonso Pena, São José dos Pinhais, Brazil.

aging process, including a decrease or increase in the activities of certain antioxidant enzymes and molecules.[9]

Invasive techniques, such as tape stripping and biopsy, provide fundamental knowledge about the skin and the effects of skin products.[10–12] However, such invasive methods lead to changes in the molecular composition of the tissue, limiting monitoring of structural and biochemical changes caused by chronological, natural aging and induced, external aging. To overcome these disadvantages, optical techniques, such as optical coherence tomography (OCT) and Raman spectroscopy, have been widely used to analyze the effects on the skin of various products designed to increase hydration and slow the aging process.[13–16] The results using these noninvasive methods are obtained in real time, in contrast to the more intrusive methods. OCT has specifically been used to study the effects of moisturizers and sunscreens on skin elasticity and hydration[17] as well as to examine structural differences among the skin of different ethnic groups.[18] However, OCT does not provide details regarding the molecular constituents and their structure conformation in a given sample.

In vivo Raman spectroscopy can identify and characterize biochemical changes arising from degenerative processes in living tissues in real time. In addition to high sensitivity and specificity, this method is noninvasive and can be used to study the major constituents of the skin, such as lipids and proteins, and hydration levels.[9,17–22]

Most studies using Raman spectroscopy have analyzed the active ingredients of cosmeceuticals and their influence on skin aging. However, studies that correlated the use of cosmetic with the biochemical alterations in the skin caused by the aging process are rare. Therefore, the main goal of the current study was to analyze, by *in vivo* dispersive and Fourier Transform (FT) Raman spectroscopy, the changes in some biomolecules, such as protein structure and lipid composition, as well as to determine the quality and hydration quantity in aging skin in the absence or presence of cosmetics.

Materials and Methods

Study approval

This study was performed according to ethical guidelines and rules for research involving human subjects and was approved by the Research Ethics Committee of the University of the Vale do Paraíba (UNIVAP) (protocol H48/CEP/2008). All volunteers signed informed consent forms.

Selection criteria and procedures

In this experiment, a commercial anti-aging product was used on all volunteers, following the fabricant instructions. The *in vivo* experiments were performed on 16 women, aged 60–75 years, who were chosen for this study based on their answers to a questionnaire that we administered. The exclusion factors were prior history of or current dermatological pathologies, irritation or sensitivity to cosmetic products, pregnancy or lactation, and change of medication during the study.

Procedure for skin analysis and composition of the cosmetic

To standardize the experiments and minimize the possible interference in the Raman date from any other cosmetic product, the volunteers did not use any type of hydrating or anti-wrinkle cosmetic for 7 days before the experiment, as well as on the day of the first Raman spectroscopic measurement (T0). After 30 days (T30) and 60 days (T60) of continuous use of a cosmetic, new measurements were taken. The cosmetics composition was mainly an oil-in-water emulsion that contained plant extracts and antioxidant vitamin, a chemistry sunscreen (protection UVA/UVB), natural moisturizers from vegetable sources, amino acids, and peptides that act to increase collagen and membrane proteins (PI-0503473-6). The volunteers used 100 mL of the product twice a day for 60 days.

Before the start of each measurement, the volunteer remained in an air-conditioned environment at a temperature of $20.0 \pm 2.0°C$ and a relative humidity of $50.0 \pm 5.0\%$ for 10 min. The skin area to be analyzed was cleaned with cotton soaked in 1.5 mL of 97% ethanol.

Raman spectroscopy

Raman spectra were collected in the high (2800–3550 cm^{-1}) and low (1070–1800 cm^{-1}) wave number regions in the periorbicular right lateral eye region. A dispersive Raman system with a 785-nm excitation source was used to obtain the low frequency spectra. The excitation laser was guided through an optical fiber (EMVISION LLC, Loxahatchee, FL) coupled to a 785-nm bandpass filter in the proximal portion and a notch filter in the distal portion. The power output of the incident radiation was adjusted to 30 mW, and an integration time of 70 sec was used for each of the three points measured in the orbicularis region. The spectrometer SpectraPro-2500i (Piacton) equipped with a CCD detector (Spec10, Princeton) of 1340×400 pixels was used to collect the Raman spectrum in conjunction with WIN SPEC software.

The high-frequency region was measured using an RFS 100/S spectrometer (Bruker Optics, USA) equipped with OPUS software (version 4.2, Bruker Optics). An Nd:YAG laser with wavelength of 1064 nm was used as the excitation source and guided using optical fiber. Raman spectra were collected using a germanium (Ge) detector with 900 scans and a spectral resolution of 4 cm^{-1}. Measurements were made at two separate points in the same facial region. The laser power applied to the skin surface was set to 70 mW.

Data processing

To remove the intrinsic fluorescence of the skin, baseline subtraction was performed using a polynomial fitting of the date using MATLAB® 6.0 (USA) software.[23]

The software ORIGIN® 7.5 (OriginLab Corporation, USA) was used to fit the Raman bands obtained by FT-Raman (Raman with Fourier transform) and Raman dispersive systems. For the low-frequency region, data were normalized with the vibrational mode at 1445 cm^{-1} (relating to angle deformation, δCH_2, lipids, and phospholipids), whereas for the high-frequency region, the data were normalized to the peak intensity at 2936 cm^{-1} (corresponding to the stretching νCH_3 of lipids).[13,21] This normalization is based on a normal distribution, with a mean of zero and a standard deviation equal to one, and the peak that was used as a reference exhibited minimal intensity and bandwidth variation between the spectra. For the low-frequency region, principal

component analysis (PCA) was used with mean centering. Linear discriminant analysis was performed by PCA using the covariance matrix.

Results

High frequency region: FT Raman spectroscopy

To determine the hydration profile, the water to protein ratio was calculated using the integrated area relative to the 3230 cm^{-1} peak (symmetric OH stretch) and protein (CH_3 stretch) at 2936 cm^{-1}.[21] Hydration at T30 and T60 were compared with the control measurement for each volunteer at T0. Figure 1a shows the average spectrum of each group at T0, T30, and T60, and the assignment of the principal vibrational modes is described in Table 1.[24–26] The average intensity of the 3150–3350 cm^{-1} region increased from T0 to T30, whereas for T60, it showed a noticeable decrease. These intensity variations may indicate changes in bonds within the hydroxyl group dominated by O-H stretch modes. To better visualize this variation in intensity, Fig. 1b shows the difference between the spectra T30–T0 and T60–T0. To avoid overlapping with the N-H vibration of protein spectra region, the integrated subtracted spectral area was calculated in the range of 3100–3490 cm^{-1}, the region of the vibration of water v (OH). The result shows that the integrated area of T30–T0 increased by 130% as compared with the T60–T0 area. The increased change in the integrated area indicates that the number of molecules of OH increased for T30 and T60. However, the area variation for T30 was larger than for T60, showing a significant improvement of the skin hydration profile.

To understand the reduction in the integrated area of the OH region after T30 and knowing that environmental changes can have direct effects on the skin, the climate changes during measurement were analyzed. The environment suffered sudden climatic changes, and the mean relative humidity was 24.3%, according to estimates made by the meteorological station at UNIVAP—Urbanova. Additionally, the skin hydration profile during the study period was compared with the plot representing relative humidity

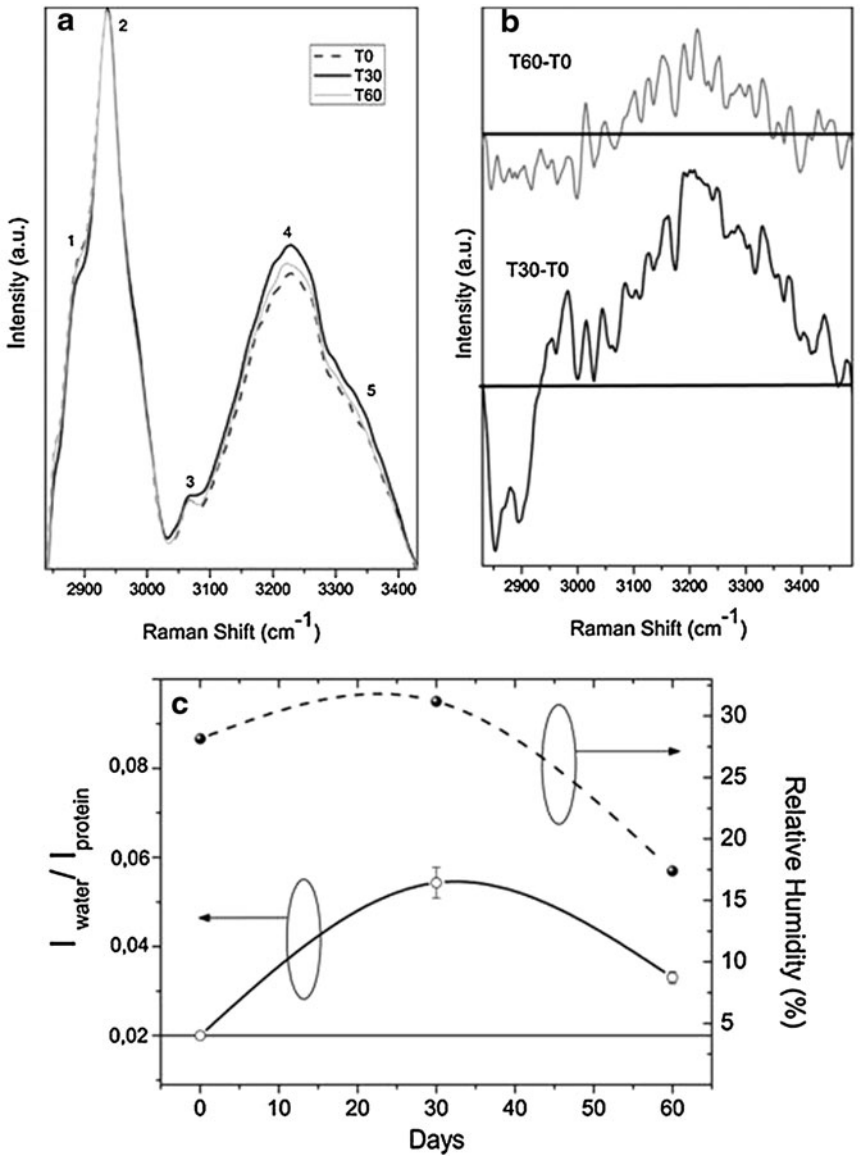

FIG. 1. **(a)** *In vivo* Raman spectrum in the spectral range of 2800–3500 cm^{-1}. The solid black line represents 30 days, the dotted black line represents the initial time, and the gray line represents 60 days. **(b)** Subtraction spectra between T30 and T60. **(c)** Comparison of the water intensity (I_{WATER}) and protein intensity ($I_{PROTEIN}$) for T60. The solid line represents the adjustment between the midpoints at T0, T30, and T60, whereas the dotted line represents the adjustment between the midpoints of relative humidity for the same period.

Table 1. Assignment of the Vibrational Spectrum of Skin at High Frequency[24–26]

Band number	Peak position (cm^{-1})	Structure	Assignment
1	2890	ν $(CH_2)_s$	Phospholipids
2	2936	ν $(CH_3)_a$	Lipids and proteins
3	3066	ν (CH)	Olefin
4	3230	ν $(OH)_s$	Water
5	3336	ν $(OH)_a$	Water

N, stretch; s, symmetrical; a, asymmetrical.

(Fig. 1c). The behavior of both curves was similar, increasing during the first 30 days of product application and then decreasing during the next 30 days, corroborating the Raman spectroscopy data in Fig. 1a.

Low frequency region: Dispersive Raman spectroscopy

Figure 2 shows the mean Raman data in the low frequency region for each of the periods measured. The main peaks, bands, and their corresponding assignments are shown in Table 2.[20,27,28] All spectra were normalized using the peak at 1445 cm^{-1}, assigned to lipids and phospholipids, which are found in large quantities in the skin. Therefore, the low variation in the intensity of this peak between the volunteers allowed it to be used for standardization. Table 2 shows that the Raman spectrum is characterized by mostly lipids and proteins (collagen), as expected for the structural composition profile of skin.

In Fig. 3a, at T30 and T60, there was an increase in the intensity of the amide III mode related to the tropocollagen, whereas the amide I mode decreased in intensity after 30 days.

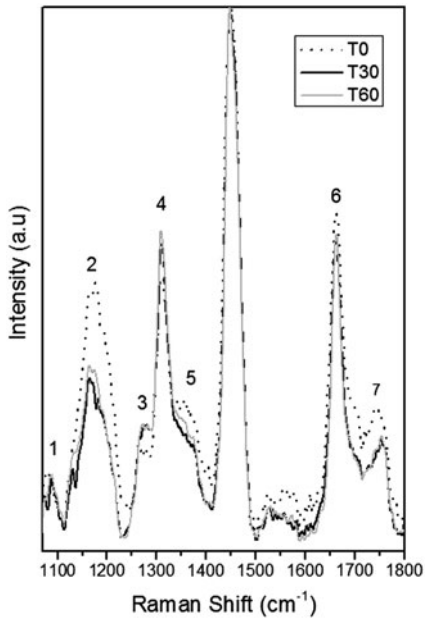

FIG. 2. *In vivo* Raman spectra in the spectral range of 1070–1800 cm^{-1}. The solid black line represents the initial measurement (T0), the dotted black line represents 30 days (T30), and the gray line represents 60 days (T60).

Table 2. Assignment of the Vibrational Spectrum of Skin at Low Frequency[20,27,28]

Band number	Peak position (cm^{-1})	Structure	Assignment
1	1083	ν (C-O)	Lipids (ceramides)
2	1170	ν $(C\text{-}O\text{-}C)_s$, ν (C-C), ρ (CH_3)	Lipids
3	1274	C=O	α-Helix amide III
4	1310	CH, NH	Amide III
5	1360	C=C, δ (CH)	Proteins
6	1659	ν (C=O), ν (C-N)	Amide I (collagen)
7	1748	ν (C=O)	Ester (triglycerides)

v, stretch; s, symmetrical.

To verify the major changes around the Raman peaks of interest, we calculated the first derivative spectra average for T0, T30, and T60. Figure 3a shows the changes in the CH_2 group and the amide III modes identified in this region, which showed a marked doublet for T0, which decreased for T30 and virtually disappeared for T60. In this range the bands at 1258 and 1303 cm^{-1} are attributed to amide III vibrations of proline-rich (nonpolar) and proline-poor (polar) regions of tropocollagen (the precursor of collagen), respectively. Changes in the ratio of these two bands have been correlated with collagen degradation.[29]

Figure 3b shows the spectral range from 1621 to 1725 cm^{-1}, indicating changes in two regions: from 1630 to 1664 cm^{-1} (Region 1) and from 1712 to 1725 cm^{-1} (Region 2) related to amide I and to triglycerides, respectively. In Region 1, one of the most notable features is the presence of a doublet peak centered at 1650 cm^{-1} for T0, which is smeared out for T30 and T60. The region around 1659 cm^{-1} is associated with collagen, with the triple-stranded helix stabilized by a large number of interchain hydrogen bonds.[29] Fourier transform infrared (FTIR) spectroscopy has already beam used to assess band displacement in the 1652–1658 cm^{-1} region, which indicates rupture of the triple helix molecule within the collagen macromolecule beyond the emergence of the 1717 cm^{-1} peak for degradation of collagen type IV by the metalloproteinase (MMP) trypsin.[30]

The absolute and relative changes in the amount of the lipids (*trans* and *gauche*) and amides were estimated using the following procedure: the integrated band area from 1076 to 1092 cm^{-1} for lipids *trans*; the integrated area from 1108 to 1131 cm^{-1} for lipids *gauche*; the integrated area from 1283 to 1308 cm^{-1} for amide III; and the integrated area from 1628 to 1666 cm^{-1} for amide I.[23] The mean and the standard error were calculated. The relative percentages of the quantity variation for each biomolecule are shown in Table 3.

As seen in Table 3, the lipids *trans* presents an increase of 62.5%, in the ceramides concentration for T30 as well as for T60. Furthermore, the concentration of lipids *gauche* decreased about 25% and 21.4% for T30 and T60, respectively.

To achieve a qualitative understanding of the data, PCA was performed on the whole spectral range for all 48 Raman spectra. Figure 3c shows the scatterplot of PC3 versus PC4, indicating two distinct groupings of spectra. The grouping on the left contained mostly the spectra of T30 and T60 separated along the PC3, whereas the group on the right contained the spectra obtained at T0 and were separated

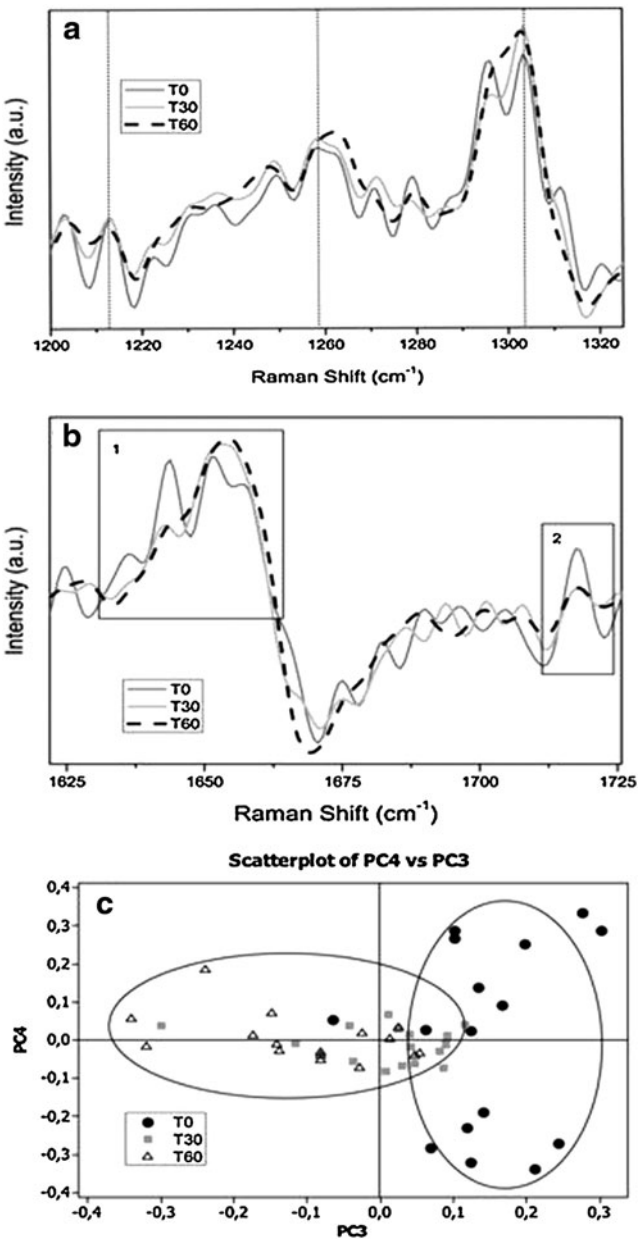

FIG. 3. **(a)** Spectral region of 1200–1325 cm^{-1} for the first derivative. The main peaks relate to amide III. **(b)** Spectral region of 1621–1725 cm^{-1} for the first derivative. Region 1 is related to amide I vibrational modes, and Region 2 is related to the triglyceride vibrational modes. **(c)** Scatterplot of PC3 vs. PC4 for all 48 spectra in all three periods (T0, T30 and T60).

Table 4. Linear Discriminant Analysis

Linear discriminant analysis (%)			
Classification group	*True group*		
	T0	T30	T60
T0	100.0	0.0	0.0
T30	0.0	70.0	30.0
T60	0.0	16.6	83.4
Total	100.0	87.5	62.5

along PC4. Another difference is that the spectra of T0 are more dispersed, whereas the spectra of T30 and T60 are more uniform and, with less variability between them. Using the first five principal components (PC1, PC2, PC3, PC4 and PC5), linear discriminant analysis was used to identify the probability of spectra belonging to each group (Table 4). All spectra of the first measurement (T0) showed 100% discrimination, indicating that all were classified within the same group. Meanwhile, the spectra of T30 showed 87.5% discrimination, and of a total of 16 spectra, only two were classified as T60. After 60 days of using the product (T60), the discriminant percentage decreased to 62.5%, with six spectra classified as T30. Interestingly, no spectrum of T30 or T60 was classified as T0. This indicates that there was differentiation between the first spectral measure when the volunteer did not use the product, and 30 or 60 days after using the cosmetic.

Discussion

The goal of this study was to evaluate any possible enhancing effects caused by commercial products on the human skin.

High frequency region: FT Raman spectroscopy

The high-frequency Raman region in Fig. 1b clearly demonstrates how a change in relative humidity influences skin hydration. Low humidity increases water evaporation from the skin because the hydrolipidic mantle, the surface layer of water and lipids, is flawed. This water loss is aggravated by several factors, including aging. However, cosmetic products containing active moisturizers are designed to prevent water loss, reducing dryness and subsequent skin flaking.[31–33] In addition to protecting the skin, the continuous use of such cosmetic products also maintains the skin's water balance, even after severe environmental changes such as low relative humidity, excess heat, and wind.[34] This effect is depicted in Fig. 1c at T30, which shows significant improvement in comparison to the relative dehydration at T0.

Table 3. Absolute (a.u.) and Relative (%) Intensity Values of Peak Area for Lipids *Trans* and *Gauche* and Amides I and III

	T0	*T30*	*T60*	*T30/T0*	*T60/T0*
Lipids *trans* (1076–1092 cm^{-1})	0.08 ± 0.02	0.13 ± 0.04	0.13 ± 0.04	62.5	62.5
Lipids *gauche* (1108–1131 cm^{-1})	0.28 ± 0.15	0.21 ± 0.07	0.22 ± 0.06	−25.0	−21.4
Amide III (1283–1308 cm^{-1})	0.43 ± 0.13	0.39 ± 0.08	0.40 ± 0.08	−9.3	−7.0
Amide I (1628–1666 cm^{-1})	1.40 ± 0.23	1.59 ± 0.19	1.66 ± 0.23	13.6	18.6

This shows the possible protective effects of skin hydration with the application of the commercial cosmetic products used in this experiment. There was also a direct proportional relationship between the CH_2 group of the phospholipids at $2890\,cm^{-1}$ and the OH group at $3250\,cm^{-1}$. This finding indicates that when water concentration increases in the skin, there is also an increase in the phospholipid levels, because these components prevent water loss.[35,36]

Low frequency region: Dispersive Raman spectroscopy

The smeared out of the doublet peak that occur in the region around $1659\,cm^{-1}$ may be explained by structural modification of the amide group after using the cosmetic product. Because the Amide I stretching mode (C=O)is weakly coupled to the stretching mode of the carbon–nitrogen bond and to the in-plane deformation mode of the nitrogen–hydrogen amide bond, the changes in the molecular geometry by the degradation of collagen triple helix chain may result in the dissociation of the triple helix into a simple string or a double string[37,38] because of changes in the peptide bonds of the secondary structure. This collagen degradation in T0, may be caused by MMPs that act on the extracellular matrix, which is composed of collagen (types I and III), elastin, proteoglycans, and fibronectins.

The amount of functional collagen and amide I in the skin increased after T60. This effect is important, because the increase of collagen quantity is not always related to the improvement of skin rigidity, but the conformation of the molecules is more important to suppress the aging skin effects. Therefore, the increase of the functional collagen is more important, because of its organized fiber state leading to better extracellular matrix organization.

In this work, it was found that there was an increase in the amount of lipids *trans* conformation from the use of the cosmetic. In almost the same proportion, there was a decrease in the lipids *gauche* that represented a disordered structure with less functionality in the extracellular matrix. The ceramides were related to the organized lipids in the extracelular matrix and therefore, the product acts by decreasing the amount of lipid that is not functional.

Conclusions

The results of this experiment demonstrate that Raman spectroscopy can detect sensitive variations of biomolecules in skin. Additionally, the data indicate that the application of cosmetics with active moisturizing and anti-aging properties helps to maintain the skin's protective barrier, maintaining hydration and slowing the intrinsic and extrinsic aging processes. Lipids, collagen, and water, considered the main components of skin, showed significant changes, even in elderly volunteers.

In both the low-frequency region, which indirectly analyzed biomolecules related to the cellular aging process, such as collagen, lipids, and MMPs, and the high-frequency region, which analyzed the percentage of water, the effects of the cosmetic were greatest at T30. Generally, T60 showed increases in the collagen and water bands demonstrating the effect of treatment with the cosmetic product. Decreases in other bands may be related to the organization of the epidermis in the dermal matrix, resulting in greater adhesion to the extracellular matrix.

It should be noted that after 30 days of treatment, depending upon their age, the volunteers may use the product less frequently or stop use once improvement of the skin becomes visually apparent. Changes in climate may also have affected the study's results, as was previously discussed.

These findings highlight the efficacy of the examined cosmetic products and demonstrate that Raman spectroscopy is an effective technique for analyzing processes occurring in aging skin.

Acknowledgments

We thank Fundação de Amparo à Pesquisa do Estado de São Paulo (FAPESP) (01/14384-8), Conselho Nacional de Desenvolvimento Cientifico e Tecnológico (CNPq) (302761/2009-8), and O Boticário for supporting this work.

Author Disclosure Statement

Priscila F.C. Menezes, Klésia Morais da Silva Belletti, Carlos Eduardo O. Praes declare a conflict of interest because they work for the company that manufactures the product on which this research was conducted.

References

1. Fuchs, J., and Packer, L. (1991). Oxidative stress, in: *Oxidants and Antioxidants*. H. Sies (ed.). London: Academic Press Limited, pp. 559–583.
2. Bronaugh, R., and Collier, S. (1993). In vitro methods for measuring skin permeation, in: *Skin Permeation: Fundamentals and Application*. J.L. Zatz (ed.). Wheaton: Allured Publishing Corp. pp. 93–115.
3. Sommer, A.P., Zhu, D., and Scharnweber, T. (2010). Laser modulated transmembrane convection: Implementation in cancer chemotherapy. J. Control. Release 148, 131–134.
4. Sommer, A.P., Zhu, D., Mester, A.R., and Försterling, H.D. (2011). Pulsed laser light forces cancer cells to absorb anticancer drugs–the role of water in nanomedicine. Artif. Cells Blood Substit. Immobil. Biotechnol. 39, 169–173.
5. Quiroga, R.M. (2005). Cosmetic Dermatology, in: *Anti-aging Medicine as it Relates to Dermatology*. C.M. Burgess (ed.). Berlin: Springer, pp. 2–14.
6. Chung, J.H., Seo, J.Y., Choi, H.R., et al. (2001). Modulation of skin collagen metabolism in aged and photoaged human skin *in vivo*. J. Invest. Dermatol. 117, 1218–1224.
7. Gniadecka, M., Nielsen, O.F., Christensen, D.H., and Wulf, H.C. (1998). Structure of water, proteins and lipids in intact human skin, hair and nail. J. Invest. Dermatol. 110, 393–398.
8. Pons, L. (2004). Estrato Córneo: Aspectos relacionados con su hidratación y permeabilidad (Stratum Corneum: Aspects related to their hydration and permeability[In Spanish]). Offarm. 23, 166–168.
9. Rhie, G., Shin, M.H., Seo, J.Y., et al (2001). Aging and photoaging-dependent changes of enzymic and nonenzymic antioxidants in the epidermis and dermis of human skin *in vivo*. J. Invest. Dermatol. 117, 1212–1217.
10. Boncheva, M., Tay, F.H., and Kazarian, S.G. (2008). Application of attenuated total reflection Fourier transform infrared imaging and tape-stripping to investigate the three-dimensional distribution of exogenous chemicals and the molecular organization in *stratum corneum*. J. Biomed. Opt. 13, 064009–17.
11. Boncheva, M., Sterke, J., Caspers, P.J., and Puppels, G.J. (2009). Depth profiling of Stratum corneum hydration *in vivo*:

a comparison between conductance and confocal Raman spectroscopic measurements. Exp. Dermatol. 18, 870–876.
12. Quatresooz, P., and Piérard, G.E. (2009). Immunohistochemical clues at aging of the skin microvascular unit. J. Cutan. Pathol. 36, 39–43.
13. Orth, D.S., and Appa, Y. (2000). Glycerine: a natural ingredient for moisturizing skin, in: *Dry Skin and Moisturizers: Chemistry and Function*. M. Loden and H.I. Maibach, (eds.). New York: Boca Raton CRC Press, pp. 213–228.
14. Tfayli, A., Piot, O., Pitre, F., and Manfait, M. (2007). Follow-up of drug permeation through excised human skin with confocal Raman microspectroscopy. Eur. Biophys. J. 8, 1049–1058.
15. Milan, A.L.K., Milão. D., Souto, A.A., and Corte, T.W.F. (2007). Estudo da hidratação da pele por emulsões cosméticas para xerose e sua estabilidade por reologia (Study of hydration skin by the cosmetics emulsions for xerosis and their stability by rheology [in Portuguese]). Braz. J. Pharmacol. Sci. 43, 649– 657.
16. Chrit, L., Bastien, P., Biatry, B., et al (2007). In vitro and *in vivo* confocal Raman study of human skin hydration: assessment of a new moisturizing agent, pMPC. Biopolymers 85, 359–369.
17. Lademann, J., Knüttel, A., Richter, H., et al (2005). Application of optical coherent tomography for skin diagnostics. Laser Phys. 15, 288–294.
18. Querleux, B., Baldeweck, T., Diridollou, S., et al (2009). Skin from various ethnic origins and aging: an *in vivo* cross-sectional multimodality imaging study. Skin Res. Technol. 15, 306–313.
19. Leikin, S., Parsegian, V.A., Yang, W.-H., and Walrafen, G.E. (1997). Raman spectral evidence for hydration forces between collagen triple helices. Biophys. 94 11,312–11,317.
20. Caspers, P.J., Lucassen, G.W., Wolthuis, R., Bruining, H.A., and Puppels, G.J. (1999). *In vitro* and *in vivo* Raman spectroscopy of human skin. Bioespectrosc. 4, 31–39.
21. Chrit, L., Hadjur, C., Morel, S. et al. (2005). *In vivo* chemical investigation of human skin using a confocal Raman fiber optic microprobe. J. Biomed. Opt. 10, 044007-1–044007-11.
22. Marvin, D., Patzelt, A., Gehse, S. et al. (2008). Cutaneous concentration of lycopene correlates significantly with the roughness of the skin. Eur. J. Pharm. Biopharm. 69, 943–947.
23. Jansen, A.M., and Kortum, R.R. (1996). Raman Spectroscopy for the detection of cancers and precancers. J. Biomed. Opt. 1, 31–70.
24. Caspers, P.J., Lucassen, G.W., Bruining, H.A., and Puppels, G.J. (2000). Automated depth-scanning confocal Raman microspectrometer for rapid *in vivo* determination of water concentration profiles in human skin. J. Raman Spectrosc. 31, 813–818.
25. Caspers, P.J., Lucassen, G.W., Carter, E.A., Bruining, H.A., and Puppels, G.J., (2001). *In vivo* confocal Raman microspectroscopy of the skin: noninvasive determination of molecular concentration profiles. J. Invest. Dermatol. 116, 434– 441.
26. Egawa, M., and Kajikawa, T. (2009). Changes in the depth profile of water in the stratum corneum treated with water. Skin Res.Technol. 15, 242–249.
27. Tfayli, A., Piot. O., and Draux. F. (2007). Molecular Characterization of reconstructed skin model by Raman microspectroscopy: comparison with excised human skin. Biopolymers 87, 261–274.
28. Penteado, S.C., Fogazza, B.P., Carvalho, C.S., et al. (2008). Diagnosis of degenerative lesions of supraspinatus rotator cuff tendons by Fourier Transform-Raman spectroscopy. J. Biomed. Opti.13, 014018-1 – 014018-10.
29. Ly, E., Piot, O., Durlach, A., Bernard, P., and Manfait, M. (2008). Polarized Raman microspectroscopy can reveal structural changes of peritumoral dermis in basal cell carcinoma. Appl. Spectrosc. 62, 1088–1094.
30. Federman, S., Miller, L.M., and Sagi, I. (2002). Following matrix metalloproteinases activity near the cell boundary by infrared micro-spectroscopy. Matrix Biol. 21, 567–577.
31. Rawlings, A.V., Scott, I.R., Harding, C.R., and Bowser, P.A. (1994). Stratum corneum moisturization at the molecular level. J. Invest. Dermatol. 103, 731–740.
32. Lóden, M., and Wessman, C. (2001). The Influence of a cream containing 20% glycerin and its vehicle on skin barrier properties. Int. J. Cosmet. Sci. 23, 115–119.
33. Crowther, J.M., Sieg, A., Blenkiron, P. et al (2008). Measuring the effects of topical moisturizers on changes in stratum corneum thickness, water gradients and hydration *in vivo*. Br. J. Dermatol. 159, 567–577.
34. Cheng, Y., Dong, Y-y., Dong, M-x., et al (2008). Protection effect of cosmetics on human skin under simulated rigorous environment. Skin Res. Technol. 14, 45–52.
35. Lóden, M., Andersson, A.C., and Lindberg, M. (1999). Improvement in skin barrier function in patients with atopic dermatitis after treatment with a moisturizing cream (Canoderm®). Br. J. Dermatol. 140, 264–267.
36. Sator, P.G., Schmidt, J.B., and Hönigsmann, H. (2003). Comparison of epidermal hydration and skin surface lipids in healthy individuals and in patients with atopic dermatitis. J. Am. Acad. Dermatol. 48, 352–358.
37. Choi, J-H., and Cho, M. (2009). Calculations of intermode coupling constants and simulations of amide I, II, and III vibrational spectra of dipeptides. Chem. Phys. 361, 168–175.
38. Gniadecka, M., Nielsen, O.F., Wessel, S., Heidenheim, M., Christensen, D.H., and Wulf, H.C. (1998). Water and protein structure in photoaged and chronically aged skin. J. Invest. Dermatol. 111, 1129–1132.

Address correspondence to:
Airton A. Martin
Instituto de Pesquisa e Desenvolvimento
Laboratório de Espectroscopia Vibracional Biomédica
Universidade do Vale do Paraíba- UNIVAP
Av. Shishima Hifumi, 2911
Urbanova, São José dos Campos
SP, 12.244-000
Brazil

E-mail: amartin@univap.br